Design of Perforated Shell Dryings Drums

Heikki Martikka[1] & Erkki Taitokari[2]

[1] Himtech Oy, Engineering, Ollintie 4, Joutseno, Finland

[2] Oy Scan Fibre Ltd, Liisakatu 26, FIN-55100 Imatra, Finland

Correspondence: Heikki Martikka, Himtech Oy, Engineering, Ollintie 4, Joutseno FIN-54100, Finland. Tel: 358-408-393-167. E-mail: heikki.martikka@pp.inet.fi

Abstract

In this study the results of optimum design of perforated cylindrical shell dryings drums are considered. These drums are used for pressurised drying of wet mass. They are important also in filter technology in macro, micro and nanoscales. The goal is formulated as maximisation of customer satisfaction on the most important decision variables. These are the fatigue endurance measured by crack propagation life, rate of water removal from mass through holes, risk of crack initiation and total cost. For perforated cylinders and plates basic engineering models are developed to get loads on the drum and to get equivalent material models to be used cost effectively in FEM. The validity of the surrogate models is tested using detailed FEM models. The results give a reasonable trade-off between many contradictory requirements. One optimal geometry is obtained and the softer steel is preferable due to better fatigue endurance and lower costs. Different surrogate models apply for static and dynamic loading.

Keywords: perforated cylinders, equivalent models, optimal fuzzy design, drum drying

1. Introduction

The use of multi-holed or perforated plates and shells is important in process industry and in heat exchangers, drying drums and energy production. Perforated shells are important in the processing industry when wet masses need to be dried in a continuous process. The material to be dried may be wood chips or pulp mass, biomass, fabric, inorganic granular materials. Various wetness removal methods include gravity, centrifugal forces, mechanical pressure, vibration, under pressure, hot air flows. Water removal by mechanical pressure can be more cost effective than by evaporation. The shells are subjected to large static and dynamic and contact loads. Their manufacturing is costly and produces inevitably some initial cracks at welds and at hole edges.

The goal has been set to design large scale structures using equivalent material models which give accurate enough stress strain results in static and dynamic loading. The equivalent elastic constant can be chosen to give the same strain as the original solid material under the same load. This concept is used by (Slot & O'Donnell, 1971). Jhung and Jo (2006) have derived equivalent elastic modules and Poisson's ratio for use in FEM modal analysis of perforated circular plates. They determined the natural frequency in air and from it the Poisson's ratio. Now static analysis is used to get the equivalent elastic modulus, wall thickness and from these the actual ligament maximum stress. The results found by (Slot et al., 1971) and (Jhung & Jo, 2006) are reliable within their ranges of validity. The theory discussed by (Gibson & Ashby, 1997) can be used to derive equivalent material properties for cellular structures. The perforated materials are a mixture of metal and holes and thus they are a member of a broad class of composites. Now the plate is an orthotropic material.

For steels the fatigue endurance is important and the models of (Gurney, 1978) are useful to evaluate differences in fatigue life between steels of different strengths. Analytical models for plates are discussed by (Szilard, 1975) and (Ventsel & Krauthammer, 2001). Now a case study of a drying rotating drum is considered. Wet mass is fed inside and compressed between inner drum and the perforated shell. Water flows out through the holes and the dried mass is conveyed out. The goal is to obtain optimal dryness with satisfactory fatigue life. The optimum design method used by as (Martikka & Pöllänen, 2009) and (Pöllänen & Martikka, 2010) is applied. It is based on the results of (Diaz, 1988). The concept and surrogate models accuracy are checked using FEM.

2. Basics of a Drying Drum Case Study

2.1 Geometry of the Case Study Drum
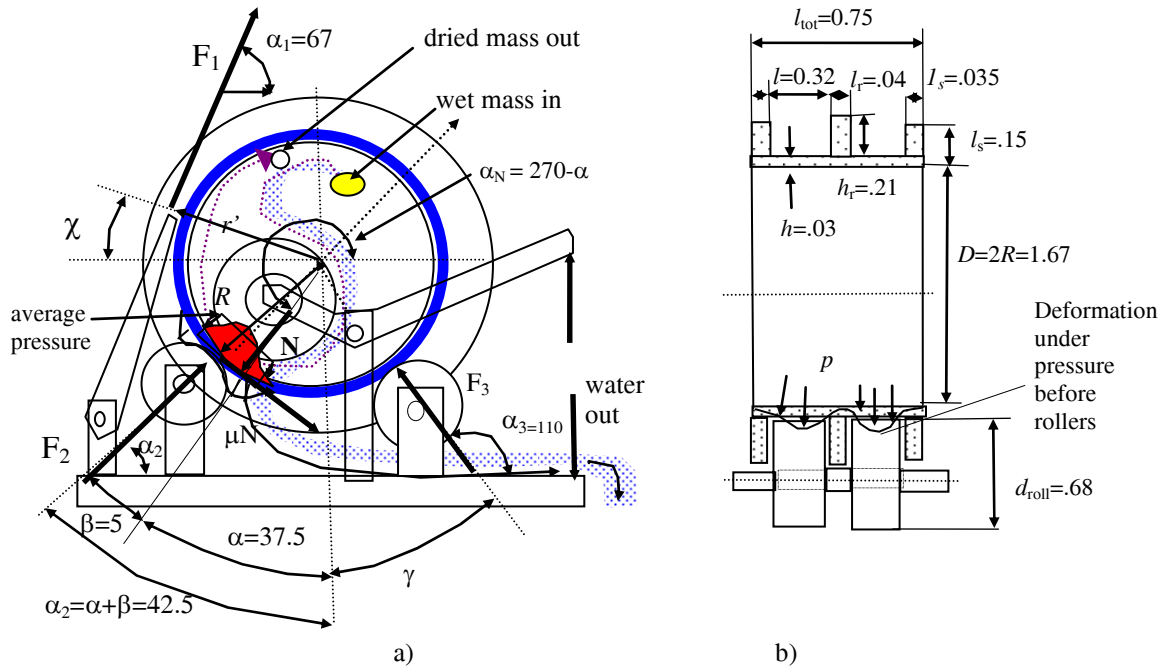
Basic geometry and loads are shown in Figure 1.

Figure 1. Basic model: a) Geometry and loads; b) Side view. Average pressure p=1.7MPa

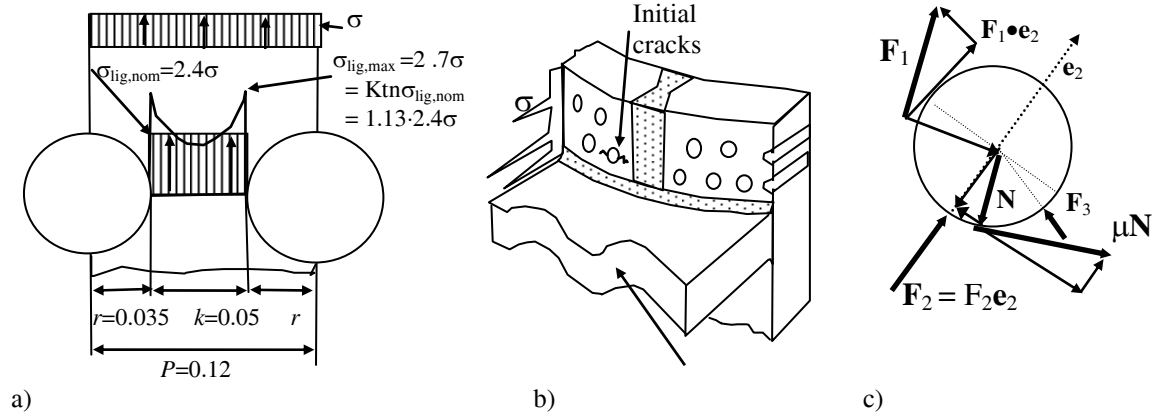Dimensions, stress and force loads are shown in Figure 2.

Figure 2. Perforated shell structure: a) Dimensions. b) Fracture locations. c) Free body model for the drum shell

2.2 Simple Stress-strain Models for Perforated Plates

Simple models can be derived using basic mechanics. A plate with regularly spaced circular perforation can be approximated by a grid type model, Figure 3. The ligament efficiency η is defined as

$$P = 2r + k \Rightarrow \eta = \frac{k}{P} = 1 - 2\frac{r}{P} \rightarrow \frac{2r}{k} = \frac{P}{k} - 1 = \frac{1}{\eta} - 1 \tag{1}$$
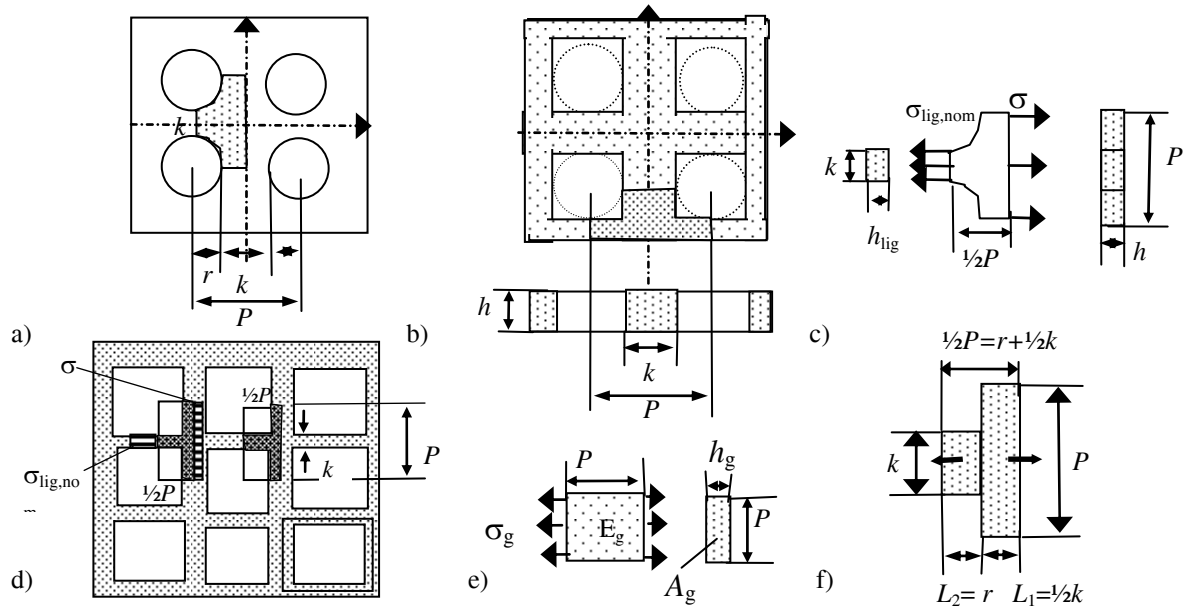
Figure 3. Material models: a) Basic model; b) Grid model from the plate with rectangular circular holes; c) FBD model for a ligament mosaic; d) Grid model with a FBD; e) Surrogate material; f) Two springs model

2.3 Force Equilibrium in Axial Direction of Drum Using Free Body Models

The FBD model in Figure 3c gives the force balance

$$\Sigma F_x = -\sigma\, hP + \sigma_{\text{lig,nom}} h_{lig} k = 0 \tag{2}$$

Here σ is the nominal stress acting plate area hP, h is the actual thickness and P is width. The ligament thickness h_{lig} is now equated to the plate thickness h since they refer to the same plate

$$h_{lig} = h \tag{3}$$

The surrogate model geometry and material properties can be defined in various ways depending on the chosen design goals. Now the thickness and elastic modulus are chosen as variables

$$h_g \neq h E_g \neq E \tag{4}$$

They are determined by FBD statics and Hooke's law. The same force is transmitted by all models

$$F = \sigma A = \sigma_g A_g = \sigma_{\text{lig,nom}} A_{\text{lig}}$$
$$F = \sigma Ph = \sigma_g Ph_g = \sigma_{\text{lig,nom}} kh \Rightarrow A = Ph, A_g = Ph_g, A_{\text{lig}} = kh \tag{5}$$

Here σ_g is the stress at the surrogate material. The nominal ligament stress $\sigma_{\text{lig,nom}}$ is higher than the nominal stress σ on solid material. It is by Figure 3c and Equation (5)

$$\sigma_{\text{lig,nom}} = \sigma \frac{P}{k} = \sigma \frac{1}{\eta} \tag{6}$$

The Equation (5) gives the surrogate plate stress σ_g

$$\sigma_g = \sigma \frac{h}{h_g} \tag{7}$$

Using Hooke's law one obtains one Equation with three unknowns defining the fictive surrogate material and plate thickness. Two more Equations are needed.

$$E \varepsilon h = E_g \varepsilon_g h_g \qquad (8)$$

The strain is one important variable. One convenient and feasible choice to define the surrogate material g is to require that it gives the same strain as the original solid material

$$\varepsilon = \varepsilon_g \qquad (9)$$

Using this in Equation (9) one obtains an equation for two unknowns.

$$E h = E_g h_g \qquad (10)$$

The surrogate elastic modulus E_g of the perforated shell can be obtained by using a model for two rod springs in series as in Figure 3f

$$\frac{1}{k_g} = \frac{1}{k_1} + \frac{1}{k_2}, \ k_1 = \frac{EA_1}{L_1} = \frac{EPh}{\frac{1}{2}k}, \ k_2 = \frac{EA_2}{L_2} = \frac{EPk}{r} \Rightarrow$$

$$\frac{k_1}{k_2} = \frac{L_2}{L_1} \frac{A_1}{A_2} = \frac{r}{\frac{1}{2}k} \frac{Ph}{Pk} = 2\frac{r}{k} \cdot \frac{P}{k} = \left(\frac{P}{k} - 1\right)\frac{P}{k} = \left(\frac{1}{\eta} - 1\right)\frac{1}{\eta} \qquad (11)$$

From this the surrogate spring constant is obtained and from it the surrogate elastic modulus

$$k_g = \frac{EA_1}{L_1}\left[\frac{1}{1 + \dfrac{k_1}{k_2}}\right] = \frac{E_g A_g}{L_g} = \frac{E_g A_1}{L_1 + L_2}, \ \Rightarrow \frac{L_g}{L_1} = \frac{\frac{1}{2}P}{\frac{1}{2}k} = \frac{1}{\eta}$$

$$E_g = E\left[\frac{\eta}{\eta^2 - \eta + 1}\right] \approx \eta E \Rightarrow \frac{E_g}{E} \approx \eta \qquad (12)$$

Now the definition of ligament efficiency is used to relate the thickness and elastic modulus ratios

$$\frac{h}{h_g} = \frac{E_g}{E} = \eta \Rightarrow h_g = \frac{1}{\eta}h, \ E_g = \eta E, \ \sigma_g = \eta \sigma \qquad (13)$$

This can be used in the FEM models of the perforated cylinder shell. From Equation (6) and Equation (13) the nominal ligament stress $\sigma_{lig,nom}$ can be obtained using the surrogate stress concept

$$\sigma_{lig,nom} = \frac{1}{\eta}\sigma = \frac{1}{\eta} \cdot \sigma_g \frac{1}{\eta} = \sigma_g \frac{1}{\eta^2} \qquad (14)$$

The maximum ligament stress $\sigma_{lig,max}$ is now obtained from the surrogate stress

$$\sigma_{lig,max} = K_t(\eta)\sigma_{lig,nom} = K_t(\eta) \cdot \frac{1}{\eta^2}\sigma_g \qquad (15)$$

Here $K_t(\eta)$ is the stress concentration factor depending to the ligament efficiency. A reasonable model for it may be obtained by data fitting to Peterson's model for a row of circular holes under tension as by (Pilkey & Pilkey, 2008). In Figure 4a the model is shown. The Neuber stress concentration is shown in Figure 4b. It is based on models by (Martikka and Pöllänen, 2010). The steel has yield stress R_p =250 and UTS R_m=360 MPa. Plastic yielding decreases the stress concentration factor to close to unity.

$$K_{t,nom}(\eta) = K_2 + (K_1 - K_2)\eta^p = K, \ K_1 = 3, \eta_1 = 1, K_2 = 1, \eta_2 = 0$$

$$\frac{\Delta K}{\Delta \eta}\big(_{\eta=1} = p\eta^{p-1}(K_1 - K_2)\big(_{\eta=1} = \frac{3-1}{1-0.35} = p(3-1) \Rightarrow p = \tfrac{1}{0.65} \qquad (16a)$$

Thus the simple model is obtained
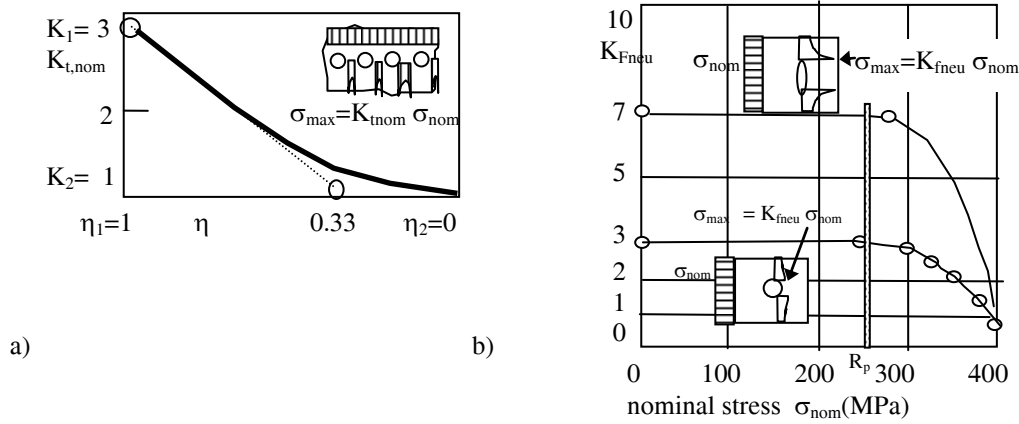
$$K(\eta) = 1 + 2\eta^{\mathrm{p}} \tag{16b}$$

Figure 4. Stress concentration models: a) Elastic stress concentration for a uniaxially stressed infinite plate with an infinite row of circular holes; Stress is perpendicular to the axis of the holes; b) Effect of plastic yielding and work hardening on the stress concentration factor of the Neuber type

As a numerical example is shown to illustrate the basic ideas and to check the logic.

A. Stress Calculation without Using the Surrogate Material Model

The stress far away from the multi-hole row is

$$\sigma = \frac{F}{A} = \frac{F}{hP} = \frac{2 \cdot 0.144\,MN}{0.042m \cdot 0.12m} = 57\,MPa \tag{17}$$

Stress concentration factor when $\eta = 0.34$ is

$$K_{t,\mathrm{nom}}(\eta) = 1 + 2\eta^{\mathrm{p}} \Rightarrow 1 + 2 \cdot 0.34^{\frac{1}{0.65}} = 1.38 \tag{18}$$

FEM results with the same models and steel material gave mean stress ate the ligament

$$\sigma_{\mathrm{lig,nom,FEM}} = \frac{F'}{kh} = \frac{0.722\,Mn}{0.020m \cdot 0.042m} = 86\,MPa \Rightarrow K_{t,\mathrm{nom,FEM}} = \frac{\sigma_{\mathrm{lig,max,FEM}}}{\sigma_{\mathrm{lig,nom,FEM}}} = \frac{113}{86} = 1.31 \tag{19}$$

When the load force is set to 2·0.144MN then this will become

$$\sigma_{\mathrm{lig,max,FEM}} = K_{t,\mathrm{nom,FEM}} \cdot \sigma_{\mathrm{lig,nom,FEM}} = 1.31 \cdot (86 \cdot 2) = 225\,MPa \tag{20}$$

The ligament nominal and maximum stresses are

$$\sigma_{\mathrm{lig,nom}} = \frac{1}{\eta}\sigma = \frac{57}{0.34} = 167\,MPa, \tag{21}$$

The maximum ligament stress is

$$\sigma_{\mathrm{lig,max}} = K_t(\eta)\sigma_{\mathrm{lig,nom}} = 1.38 \cdot 167 = 230 \tag{22}$$

This agrees with the FEM result of 225 MPa.

B. Stress Calculation Using the Surrogate Material Model to Get the Actual Maximum Stress

The same force F is applied to the surrogate plate by Equation (5). The surrogate thickness is

$$h_g = \frac{h}{\eta} = \frac{0.042m}{0.34} = 0.123m \tag{23}$$

The surrogate material stress is

$$\sigma_g = \frac{F}{A_g} = \frac{F}{h_g P} = \frac{2 \cdot 0.144\,MN}{0.123m \cdot 0.12m} = \frac{hF}{h_g Ph} = \frac{h}{h_g}\sigma = \eta\sigma = 0.34 \cdot 57 = 19.4\,MPa \tag{24}$$

The ligament maximum stress is given by Equation (14)

$$\sigma_{lig.\max} = K_t(\eta) \cdot \frac{1}{\eta^2} \cdot \sigma_g = 1.38 \cdot \frac{1}{0.34^2} \cdot 19.4 = 231 \tag{25}$$

This demonstration shows that actual stress can be obtained from the surrogate stress

2.4 Load Force and Torque Analysis Using Statics

Torque equilibrium around the axis of the drum in Figure 1a

$$\Sigma T = \mathbf{r} \times \mathbf{F}_1 + \mathbf{R} \times \mu\mathbf{N} = 0 \Rightarrow rF_1 = R\mu N \tag{26}$$

Here the friction force depends on the coefficient of friction between non-metal wet mass and metal. Generally is between 0.3...0.35. Now a realistic value is about $\mu = 0.32$. Using this normal force can be calculated as

$$F_1 = 0.3\,MN, r = 1.06, R = 0.835 \tag{27}$$

$$N = \frac{rF_1}{\mu R_1} = \frac{1.06 \cdot 0.3\,MN}{0.32 \cdot 0.835} \approx 1.2\,MN \tag{28}$$

The angles between forces are shown in Figure 1

$$\alpha = 37.5, \beta = 5, \alpha_1 = 67, \alpha_2 = \alpha + \beta = 37.5 + 5 = 42.5, \alpha_3 = 110, \alpha_N = 270 - \alpha \tag{29}$$

The friction coefficient and the compressive resultant normal force are

$$\mu = 0.32, N = 1.2MN, \tag{30}$$

Force balance can be written as

$$\Sigma\mathbf{F} = \mathbf{F}_1 + \mathbf{N} + \mu\mathbf{N} + \mathbf{F}_2 + \mathbf{F}_3 = 0 \tag{31}$$

In component form

$$F_1\begin{pmatrix}\cos\alpha_1 \\ \sin\alpha_1\end{pmatrix} + N\begin{pmatrix}\cos\alpha_N \\ \sin\alpha_N\end{pmatrix} + \mu N\begin{pmatrix}\cos\left(\alpha_N + \frac{1}{2}\pi\right) \\ \sin\left(\alpha_N + \frac{1}{2}\pi\right)\end{pmatrix} + F_2\begin{pmatrix}\cos\alpha_2 \\ \sin\alpha_2\end{pmatrix} + F_3\begin{pmatrix}\cos\alpha_3 \\ \sin\alpha_3\end{pmatrix} = 0 \tag{32}$$

Substitution of known data gives two equations with two unknowns. They can be solved from

$$0.3MN\begin{pmatrix}\cos 67 \\ \sin 67\end{pmatrix} + 1.2MN\begin{pmatrix}\cos\alpha_N \\ \sin\alpha_N\end{pmatrix} + 0.317 \cdot 1.2MN\begin{pmatrix}\cos(\alpha_N + 90) \\ \sin(\alpha_N + 90)\end{pmatrix} +$$

$$+F_2\begin{pmatrix}\cos 42.5 \\ \sin 42.5\end{pmatrix} + F_3\begin{pmatrix}\cos 110 \\ \sin 110\end{pmatrix} = 0, \alpha_N = 270 - \alpha = 270 - 37.5 \tag{33}$$

The external reaction forces due to supporting cylinders are

$$F_2 = 0.964\,MN, F_3 \approx 0 \tag{34}$$

2.5 Local Bending Model of a Tube with Mid Stiffener

Local bending line moment at the shell due to the stiffeners is

$$m = \frac{1}{2\beta^2\left[1 + 2\dfrac{h}{A_r\beta}\right]}p = \frac{pl^2}{250l^2} = \frac{1}{25}pl^2, l = 0.32, \tag{35}$$

Where

$$\beta = \left[\frac{3\left(1-\nu^2\right)}{R^2 h^2}\right]^{\frac{1}{4}} = 8\left[\tfrac{1}{m}\right], \nu = 0.3, h = 0.042m, R = 0.735m \tag{36}$$

2.6 Plate Model with Even Pressure Model

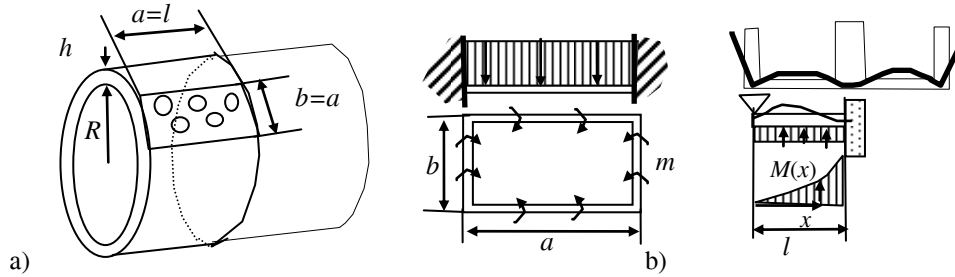A plate model with stiff supports can be applied to the locally pressured area.

Figure 5. Surrogate models: a) Cylinder with a plate model; b) Plate and beam model

According to (Szilard, 1975) the line bending moment of a plate with stiff supports at all ends is

$$m = \frac{M}{b} = c_4 p a^2 = 0.0513 p l^2 = \tfrac{1}{20} p l^2, l = 0.32, b/a = 1 \tag{37}$$

2.7 Simple Beam and Plate Models for Maximum Bending Moment

Bending moment approximations are

$$m = \frac{1}{s} p l^2 = \left(\frac{1}{8}..\frac{1}{12}..\frac{1}{20}...\frac{1}{25}\right) p l^2 \tag{38}$$

Where the model parameter s depends on the chosen approximation model

$$\begin{aligned} &s = 8, \text{beam}, \text{free} - \text{fixed.supports} \\ &s = 12, \text{beam}, \ \text{fixed} - \text{fixed} - \text{support} \\ &s = 20, \text{plate}, \text{b}/\text{a} = 1, \text{fixed} - \text{fixed} \\ &s = 25, t\text{ube. with.stiffener. ring. and. internal. pressure} \end{aligned} \tag{39}$$

The nominal bending stress depends on the moment

$$\sigma_{\mathrm{b}} = \frac{M}{W_b} = \frac{mb}{\frac{1}{6} b h^2} = \frac{m}{\frac{1}{6} h^2} = \frac{\frac{1}{s} p l^2}{\frac{1}{6} h^2} \tag{40}$$

2.8 Global Dending of a Cylinder

The dominant bending forces can be obtained by projecting all forces to $\mathbf{F}_2$ direction

$$\hat{\mathbf{e}}_2 \bullet \quad \| \quad \hat{\mathbf{e}}_1 F_1 + \hat{\mathbf{e}}_N N + \hat{\mathbf{e}}_{\mu N}\left(\mu N\right) + \hat{\mathbf{e}}_2 F_2 = 0 \tag{41}$$

In matrix form one obtains

$$\binom{\cos \alpha_2}{\sin \alpha_2} \bullet \left| F_1 \binom{\cos \alpha_1}{\sin \alpha_1} + N \binom{\cos \alpha_N}{\sin \alpha_N} + \mu N \binom{\cos\left(\alpha_N + \frac{1}{2}\pi\right)}{\sin\left(\alpha_N + \frac{1}{2}\pi\right)} + F_2 \binom{\cos \alpha_2}{\sin \alpha_2} = 0 \tag{42}$$

The result is

$$\hat{\mathbf{e}}_2 \bullet \hat{\mathbf{e}}_1 F_1 + \hat{\mathbf{e}}_2 \bullet \hat{\mathbf{e}}_N N + \hat{\mathbf{e}}_2 \bullet \hat{\mathbf{e}}_{\mu N}(\mu N) + F_2 = 0 \tag{43}$$

The force F_2 acting at the roller 2 is

$$F_2 = -\cos(\alpha_2 - \alpha_1)F_1 - \cos(\alpha_2 - \alpha_N)N - \cos\left(\alpha_2 - \alpha_N - \tfrac{1}{2}\pi\right)(\mu N) \tag{44}$$

Bending moment M (Nm) at mid point and bending stress are

$$M = \frac{F_2}{2}\frac{l}{4} , \; \sigma_{\text{bend,M}} = \frac{M}{W} = \frac{M}{\pi R^2 h} \tag{45}$$

2.9 Bending Stress to Local Pressure Bulging on the Shell

The nominal local bending stress at the ligaments is higher due to ligament efficiency factor

$$\sigma_{\text{bend,p}} = \frac{pl^2}{s\frac{1}{6}h^2} , \; \sigma_{\text{lig,nom,p}} = \frac{\sigma_{\text{bend,p}}}{\eta} \tag{46}$$

The maximal stress is higher at hole edges due to stress concentration factor $K_{\text{t,nom}}$.

$$\sigma_{\text{max,p}} = K_{\text{t,nom}}\sigma_{\text{lig,nom,p}} \tag{47}$$

3. Total Stress

The total maximum stress due to inner pressure (p) and bending moment (M) constraints is

$$\sigma_{\text{max,p}} = K_{\text{t,nom}}\frac{1}{\eta}\sigma_{\text{bend,p}} , \; \sigma_{\text{max,M}} = K_{\text{t,nom}}\frac{1}{\eta}\sigma_{\text{bend,M}} \tag{48}$$

Total maximum stress is sum of pressure and moment caused stresses

$$\sigma_{\text{max}} = \sigma_{\text{max,p}} + \sigma_{\text{max,M}} \tag{49}$$

Constructional method of increasing the fatigue life can be derived from the stress equation. The cracks start at the holes edges situated at the maximum moment. The bending moment by the beam model can be used to find safe enough locations of the holes, Figure 4c.

$$M(x) = Q\tfrac{1}{2}x\left(\tfrac{3}{4} - \tfrac{x}{l}\right) \rightarrow \frac{M(l)}{M(0.9l)} \approx 0.5 \Rightarrow X_M = 0.5 \tag{50}$$

Thus the optimal location for the fist row of holes is at 90% of the length l since there the maximum stress has decreased sufficiently from the extreme position at $x = l$. When the moment is halved the stresses also are halved and fatigue life is increased by 8 fold.

$$\sigma_{\text{max}}(0.9l) \Rightarrow \sigma_{\text{max}}(l)X_M \tag{51}$$

4. Design Variables and Goal

The design goals can advantageously expressed using fuzzy logic. One may proceed in the followings stages.

4.1 Technical and Economic Design Variables

Geometrical design variables are thickness and ligament geometry. Material variables are material classes and their properties. Functional variables are safety factors.

Table 1. Geometrical design variables options. Principle of modelling of the general satisfaction functions. Its position and skewness can be varied

index	ligament efficiency lig(ilig)=η	drum wall thickness h(ih) (m)
1	0.34	0.030
2	0.35	0.032
3	0.36	0.034
4	0.37	0.036
5	0.38	0.038
6	0.40	0.040
7	0.42	0.041
8	-	0.042

Table 2. Material variables. The Paris law C and m parameters are calculated with Gurney's (1978) model Stress ratio $R_s = \sigma_{min}/\sigma_{min} = 0$, K_{th} (N·mm$^{3/2}$)

	OX steel im = 1	St52 steel im=2
Yield strength (Pa)	Re(1) = 1E+09	Re(2) = 3.4E+08
unit cost (eur/kg)	Cm(1) = 20	Cm(2) = 5
density (kg/m^3)	rho(1) = 8000	rho(2) = 8000
ecological value	eco(1) = .1	eco(2) = .7
corrosion resistance	corres(1) = .8	corres(2) = .15
Elastic modules	E(1) = 2.1eE+11	E(2) = 2.1E+11
Threshold intensity	Kth(1) = 275	Kth(2) = 190-144 · Rs
critical crack	a0kr(1) = 1/127	a0kr(2) = 1/14.6
initial crack size	a0(1) = .1 ' mm	a0(2) = .1, mm
Paris C parameter	C(1) = 4.64E-12	C(2) = 1.67E-14
Paris m exponent	m(1) = 2.52	m(2) = 3.36

4.2 Fuzzy Goal Formulation Using Decision Variables

Any vague goal of a concept can be defined easily as maximisation of total customer satisfaction on it (A. Diaz, 1988).The total event is decision variable *s* and intersection of other decision variables s_k

$$s = s_1 \cap s_2 \cap s_3 \cap s_4 \cap s_5 \cap s_6 \qquad (52)$$

The design goal is maximisation of the total satisfaction of the customer on the product

$$P(s) \Rightarrow P(s) = P(s_1) \cdot P(s_2) \cdot ..... \cdot P(s_n) \quad , \quad Q = \max P \qquad (53)$$

Now all goals and constraints are formulated consistently by one flexible fuzzy function. This is illustrated in Table 1.

5. Decision Variables

5.1 Fatigue Life

This may defined as fatigue life N in cycles of operations in years. The fatigue life of a perforated plate depends on the third power of the ligament efficiency. The equation suggests η=1 as optimal.

$$N = \frac{C}{\sigma_{max}^3} = k\eta^3 \Rightarrow \max, \Rightarrow \eta_{opt} \Rightarrow 1 \qquad (54)$$

When the structure contains initial flaws then the fatigue life is about the same as time spent in crack growth

since initiation time is not needed. According to (Gurney, 1978) the Paris-Erdogan law is applicable,

$$\frac{da}{dN} = C\left(\Delta K\right)^{\mathrm{m}}, \Delta K = Y\Delta\sigma\sqrt{\pi a}, a_{\mathrm{f}} = \frac{1}{\pi}\left(\frac{K_{\mathrm{Ic}}}{R_{\mathrm{e}}}\right)^2 \Delta\sigma = \sigma_{\max} - \sigma_{\min} \tag{55}$$

Where

a is crack length, in mm units

ΔK is stress intensity factor range,

$\Delta\sigma$ is stress, (MPa)

Y is factor due to geometry close to crack. Now Y = 1.2, at the edge of the holes Y = K_{tn}

a_{f} is the final crack length, mm

R_{e} is yield strength and K_{Ic} is fracture toughness.

a_0 is initial crack size. It depends on steel strength. For steels with R_{m} >700, a_0 =0.015, mm and with R_{m} < 700, a_0 = 0.05mm. Now a_0 is estimated conservatively as 0.1mm.

The factor C is estimated according to (Gurney, 1978). In this model the exponent m depends on the yield strength approximately as

$$m = 600\left(R_{\mathrm{e}}[\mathrm{Pa}]\right)^{-0.264} \quad C' = \frac{A}{B^{\mathrm{m}}} \quad C = C_{\mathrm{corr}}C' \tag{56}$$

Here the parameters are $A = 131.5 \cdot 10^{-6}$, $B = 895.4$ at the stress ratio, $R_{\mathrm{s}} = \sigma_{\min}/\sigma_{\max} = 0$, C_{corr} is corrosion enhancement factor. Some rough estimates are: C_{corr} =1 with no corrosion and C_{corr} = 10 with wet corrosion.

C_{corr} increases when the surface moisture is increased from dry to 80%.

At very low ΔK values C_{corr} is 20 and at high ΔK values it is about 3.

The fatigue life in number of cycles from initial to final crack length is

$$N = \frac{1}{C\left(\frac{1}{2}m-1\right)\left(\Delta\sigma Y\sqrt{\pi}\right)^{\mathrm{m}}}\left[\frac{1}{a_0^{\frac{1}{2}m-1}} - \frac{1}{a_{\mathrm{f}}^{\frac{1}{2}m-1}}\right], s_1 = \frac{N}{10^6} \tag{57}$$

High value if s_1 is desirable

$$s_1 = N, \Rightarrow 0 = s_{1\min} < s_1 < s_{1\max} = 8, bias: p_1, p_2 = 2, 0.1 \tag{58}$$

5.2 Wetness Removal Rate

The wetness removal outflow rate Q (m³/s) depends on pressure difference and ligament efficiency

$$\frac{Q}{A} = \frac{Q}{P^2} = k\frac{d^4}{P^2} = kP^2\left(1-\eta\right)^4 = kP^2 w_{\mathrm{out}}, w_{\mathrm{out}} = \left(1-\eta\right)^4 \tag{59}$$

Here using models by (Dimarogonas & al, 1992) (p 83) for piston damper

$$k = \frac{\pi\Delta p}{128\mu h}, \quad \mu = \rho v = 996 \cdot 0.802 \cdot 10^{-3} \approx 0.8 \cdot 10^{-3}, \quad t = 30C, \quad \Delta p = p - 0 = 1.7 MPa \tag{60}$$

Large value of wet removal rate is desired

$$s_2 = w_{\mathrm{out}} = \left(1-\eta\right)^4,$$
$$0 = s_{2\min} < s_2 < s_{2\max} = 1, bias: p_1, p_2 = 0.2, 0.2 \tag{61}$$

5.3 Crack Initiation Risk

Crack propagation rate may be expressed as

$$\frac{da}{dN} = C\left(\frac{\Delta K_{\mathrm{I}}}{E}\right)^n \tag{62}$$

If the ratio in the exponent is small then the crack growth is slow

$$\Delta K = \Delta \sigma \sqrt{\pi a} \le E\left[\frac{N}{mm^2}\right]\cdot 5\cdot 10^{-4}\left[mm^{\frac{1}{2}}\right] \tag{63}$$

According to the statistical work hardening the accumulation of internal defects is small if

$$\sigma < \tfrac{2}{3}R_e$$

$$a_{0kr}(im) = \frac{1}{\pi}\left[\frac{C_{a0kr}E(im)}{\Delta\sigma}\right]^2, \Delta\sigma = \tfrac{2}{3}R_e(im), a_0 = 0.1mm \tag{64}$$

The crack initiation risk may be defined as

$$s_3 = \frac{a_0(im)}{a_{0kr}(im)}, a_0(im) = 0.1mm \tag{65}$$

Small value of s_3 is desirable although high values may be inevitable

$$0.1 = s_{3min} < s_3 < s_{3max} = 20, bias: p_1, p_2 = 0.1, 3 \tag{66}$$

5.4 Cost of Material and Manufacturing

This may defined as total cost of material including manufacturing

$$s_4 = K \Rightarrow s_{4min} < s_4 < s_{4max}, K = Cost, bias: p_1, p_2 = 0.1, 3 \tag{67}$$

Cost is defined as material cost, unit cost time the mass

$$K = cm = c\rho hP^2\left[1-\left(\frac{2r}{P}\right)^2\right], \quad \frac{2r}{P} = 1-\eta \tag{68}$$

Or

$$K = c\rho hP^2\left[1-(1-\eta)^2\right] = c\rho hP^2[\eta(2-\eta)] = K_{max}\eta(2-\eta) \tag{69}$$

6. Optimisation Results

Fatigue life may be increased by closing the nearest row of holes close to the mid parts since the bending moment at 0.9 l hole ligament will decrease to half and the fatigue life increase by 8 fold using the beam model.

Table 3. Results of optimisation. The holes start at distance $x=0.9l$ from the maximal moment. Here im = 1 denotes the high strength steel and im =2 denotes the medium strength steel

property	Ox im=1	Fe52 im=2
PG, Total satisfaction	$4.7\cdot 10^{-6}$	$6672\cdot 10^{-6}$
lig = η, ligament efficiency	0.34	0.34
h (m) wall thickness	0.042	0.042
s_1/P_{s1}, fatigue life/satisfaction	1.05/0.025	2.8/0.18
s_2/P_{s2}, wetness removal rate/satisfaction	0.19/0.05	0.19/0.05
s_3/P_{s3}, crack initiation risk/satisfaction	12.7/0.074	1.46/0.96
s_4/P_{s4}, cost/satisfaction	$6.8\cdot 10^{-5}/0.05$	$1.7\cdot 10^{-5}/0.74$

One may note the following. Total satisfaction on the drum with low strength steel was higher than with the drum with high strength steel. The satisfaction on water removal rate does not depend on the steel strength but only on the geometry. The difference in satisfaction is that the high strength steel has a low fatigue life and higher crack initiation risk and higher material cost than the low strength steel,

7. FEM Results

In FEM modelling (IDEAS) perforated surrogate model used. Wall thickness is the same $h = 0.42$ and $\eta = 0.34$ and loads are the same as previously.

7.1 Elastic Modulus and Thickness of Perforated Material

Elastic modulus and density are needed in dynamical modelling. In static calculations the material properties are not needed only loads and geometry. Same total strain and thickness are assumed

$$\eta = \frac{k}{P} = 0.34 = \frac{k}{0.12} \Rightarrow k = 0.0408, r = \tfrac{1}{2}(P - k) = \tfrac{1}{2}(0.12 - 0.04) = 0.04 \tag{70}$$

Thus surrogate elastic modulus as function of ligament strength is estimated as

$$E_g = E\left[\frac{\eta}{1 - \eta + \eta^2}\right] \approx \eta E = 0.34 \cdot 200000\, MP2 = 68000\, MPa\, \eta < 1, \tag{71}$$

The surrogate thickness is as function of ligament strength is

$$h_g = \frac{1}{\eta} h = \frac{1}{0.34} 0.042 = 0.1235 \tag{72}$$

7.2 Poisson's Ratio Estimations

When perforations are large the material approaches a grid or even a planar cellar orthotropic structure. In normal load direction loading it behaves as steel but in transverse directions as a cellular solid plate loaded at in-plane loading. Thus the reciprocity relationship may now be applied using the model by (Gibson & Ashby, 1997)

$$\nu_x = \nu_x = \nu_g = \frac{E_g}{E_z} \nu_z = \frac{68000}{20000} 0.3 = 0.1 \tag{73}$$

7.3 FEM Analysis of the Drum

FEM results are shown in Figure 6. For steel models with optimal dimensions the FEM stress concentration factor was 1.31 and the analytical rough model gave 1.38.

$$\sigma_{lig,max,FEM} = K_{t,nom,FEM} \cdot \sigma_{lig,nom,FEM} = 1.31 \cdot (86 \cdot 2) = 225\, MPa \tag{74}$$

The surrogate material was orthotropic. In the normal to surface z direction it was like steel. But in transverse x and y direction a honeycomb likes structure.

$$\begin{aligned} E_1 &= 68000\, MPa, & G_{12} &= 3091\, MPa, & \nu_{12} &= 0.1 \\ E_2 &= 68000\, MPa, & G_{23} &= 3091\, MPa, & \nu_{23} &= 0.1 \\ E_3 &= 200000\, MPa, & G_{13} &= 76923\, MPa, & \nu_{13} &= 0.3 \end{aligned} \tag{75}$$

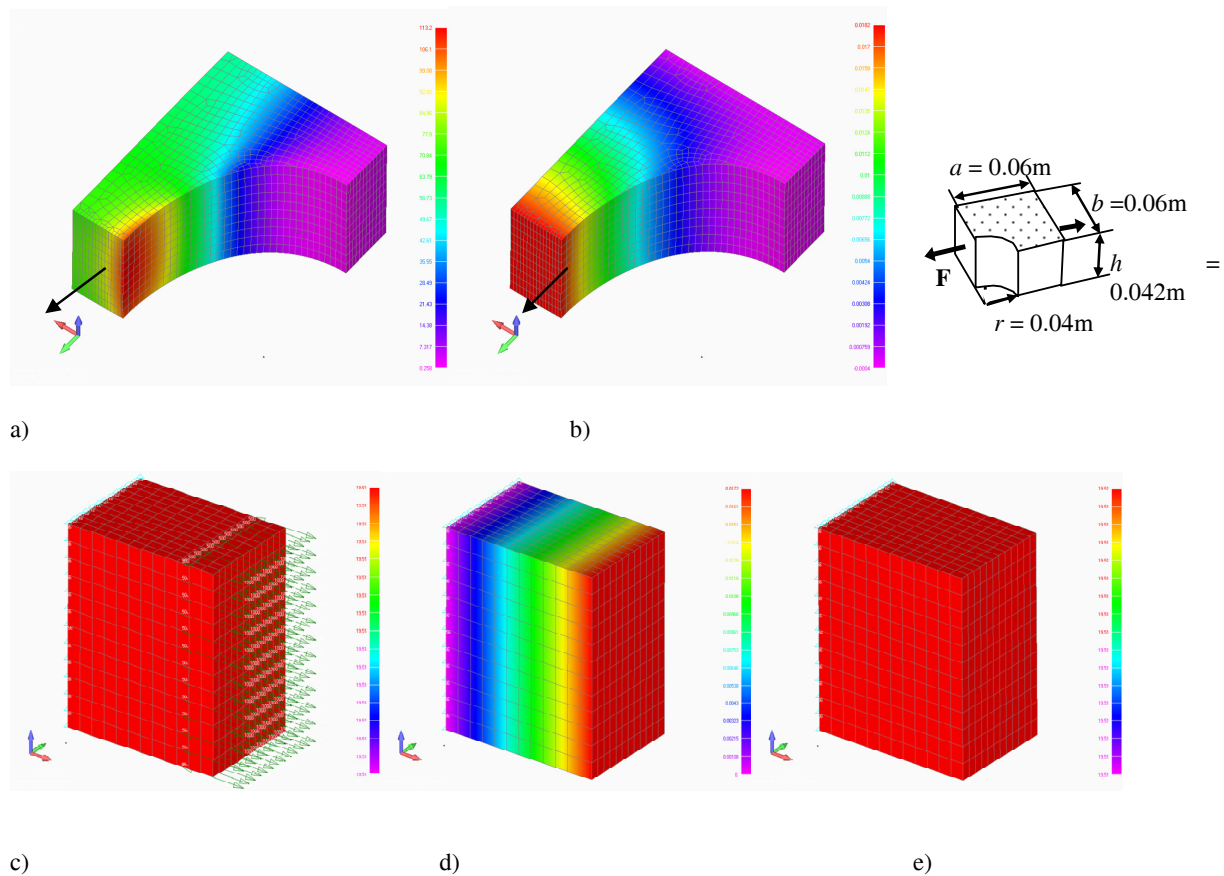The surrogate material stress by analytical model is

$$\sigma_g = \frac{F}{A_g} = \frac{F}{h_g P} = \frac{2 \cdot 0.144\, MN}{0.123m \cdot 0.12m} = \frac{hF}{h_g Ph} = \frac{h}{h_g}\sigma = \eta\sigma = 0.34 \cdot 57 = 19.4\, MPa$$

The FEM stress was calculated as principal stress.

$$\sigma_{g,FEM} = 19.51\, MPa$$

The results of the surrogate model are reasonably close to the accurate FEM result.

a)   b)

c)   d)   e)

Figure 6. FEM results: a) Actual steel model for getting the stress concentration factor; The mean tensile stress at the ligament is 86 MPa and the maximum stress is 113MPa at hole edge. Thus the nominal stress concentration factor is 1.31. The analytical estimate was 1.38; b) strains in tensile direction, max 0.0182 mm; c) The surrogate model showing boundary conditions and load of even load force distribution; Dimension in load direction is 0.06m, in transverse to load direction 0.06m and height is 0.1235 m; d) Maximum principal stress is 19.51MPa; e) Translation in the tensile direction (x) is 0.0172 mm

FEM model of the drum and picture of a typical drying drum machine are shown in Figure 7.

Figure 7. a) FEM model of the drum; b) Picture of a typical drying drum machine
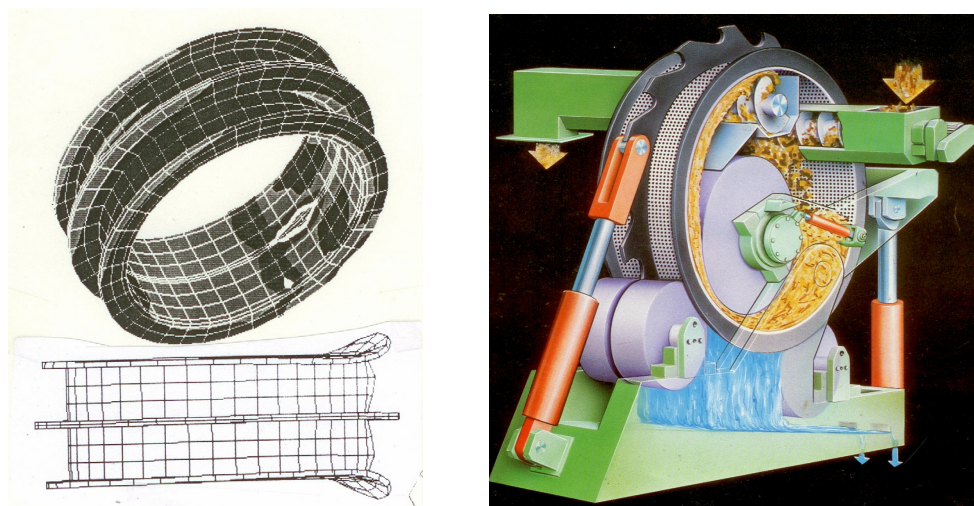
8. Conclusions

In design tasks there appear cases when the structure is macrogeometrically complex and large and the material microgeometry is also complex, like perforated shells. FEM is an efficient tool to solve such tasks. But a large amount of elements is needed and calculation times become too long with many degrees of freedom. One solution to speed up calculations is to use super elements. Another way to use FEM effectively is to use simplified homogeneous surrogate materials which are geometrically simple and give satisfactorily accurate results after a moderate simple post-processing.

One advantage of these physical simple models is that they can be used both in FEM analysis and also in concept innovation in analytical optimisation work. Another advantage is that the models are useful in concept optimisation and the stresses at critical locations are accurate enough. One disadvantage is that additional post-processing models have to be used to get strains and stresses. The other disadvantage is that the range of satisfactory accuracy needs to be considered. The future goal is to apply these methods to design of similar equipment.

References

Diaz, A. (1988). Goal aggregation in design optimization. *Engineering Optimization, 13*, 257-273. http://dx.doi.org/10.1080/03052158808940958

Dimarogonas, A. D., & Haddad, S. (1992). *Vibration for Engineers*. Prentice Hall.

Gibson, L. M., & Ashby, M. F. (1997). *Cellular solids*. Cambridge University Press.

Gurney, T. R. (1978). An analysis of some crack propagation data for steel subjected to pulsating tension loading. *The Welding Institute*, 59/1978/E. IDEAS FEM program.

Jo Jhung, Myung, & Jo, Jong Chull. (2006). Equivalent material properties of perforated plate with triangular or square penetration pattern for dynamic analysis. *Nuclear Engineering and Technology, 38*(7), 689-696.

Martikka, H. I., & Pöllänen, I. (2009). Multi-objective optimisation by technical laws and heuristics. *Memetic computing*. http://dx.doi.org/10.1007/s12293-009-0007-x

Pilkey, W. D., & Pilkey, D. F. (2008). *Peterson's Stress Concentration Factors* (3rd ed.).

Pöllänen, I., & Martikka, H. (2010). Fatigue endurance dimensioning by strain life method with a novel notch coefficient. *Machine Design, 2010*, 43-48.

Slot, T., & O'Donnell, W. J. (1971). Effective Elastic Constants for thick Perforated Plates with Triangular and Square Penetration Patterns. *Journal of Engineering for Industry, 93*(4), 935-942. http://dx.doi.org/10.1115/1.3428087

Szilard, R. (1975). *Theory and Analysis of Plates*. USA: Prentice-Hall.

Ventsel, E., & Krauthammer, T. (2001). *Thin Plates and shells*. New York, NY: Marcel Dekker. http://dx.doi.org/10.1201/9780203908723